# Quantum entanglement in two-electron atomic models

**D Manzano[1,2], A R Plastino[1,3], J S Dehesa[1,2] and T Koga[4]**

[1] Instituto Carlos I de Física Teórica y Computacional, Universidad de Granada,
Granada E-18071, Spain
[2] Departamento de Física Atómica, Molecular y Nuclear, Universidad de Granada,
Granada E-18071, Spain
[3] National University La Plata, UNLP-CREG-CONICET, C.C. 727, La Plata 1900, Argentina
[4] Applied Chemistry Research Unit, Graduate School of Engineering, Muroran Institute of
Technology, Muroran, Hokkaido 050-8585, Japan

E-mail: arplastino@ugr.es

### Abstract
We explore the main entanglement properties exhibited by the eigenfunctions
of two exactly soluble two-electron models, the Crandall atom and the Hooke
atom, and compare them with the entanglement features of helium-like systems.
We compute the amount of entanglement associated with the wavefunctions
corresponding to the fundamental and first few excited states of these models.
We investigate the dependence of the entanglement on the parameters of the
models and on the quantum numbers of the eigenstates. It is found that the
amount of entanglement of the system tends to increase with energy in both
models. In addition, we study the entanglement of a few states of helium-like
systems, which we compute using high-quality Kinoshita-like eigenfunctions.
The dependence of the entanglement of helium-like atoms on the nuclear charge
and on energy is found to be consistent with the trends observed in the previous
two model systems.

PACS numbers: 03.65.−w, 03.67.−a, 03.67.Mn

(Some figures in this article are in colour only in the electronic version)

## 1. Introduction

Information-theoretic ideas and methods provide an interesting new point of view in the study
of atomic structure that has been explored in various recent research works [1–12]. This
line of enquiry has several points of contact with the field of quantum information theory,
particularly in connection with the study of the entanglement-related properties exhibited
by atomic systems. Besides its intrinsic theoretical interest, this area of research is also of

practical relevance because some of the systems studied by contemporary atomic physics, such as ion traps, constitute important candidates for the experimental implementation of quantum information technology.

Quantum entanglement is one of the most essential features of quantum mechanics [13–15]. Entanglement constitutes a fundamental resource for the implementation of quantum information processes of technological relevance, such as quantum teleportation, superdense coding and quantum computation [14, 16]. Recent developments related to the study of quantum entanglement are also leading to a more indepth understanding of various basic aspects of quantum physics, such as, for example, quantum interference [17], the foundations of quantum statistical mechanics [18] and the quantum-to-classical transition [19].

Quantum entanglement in two-electron systems has attracted the attention of several researchers [5–8, 20–22]. Interesting results concerning the entanglement-related features of the eigenstates of a one-dimensional atomic model with Coulomb-like interactions [8], the ground state of the Hooke system [20], the spherically averaged helium-like model near the ionization threshold [21] and quantum dots with a step-like confining potential well [22] have been recently reported. However, the systematic characterization of the entanglement properties of the eigenstates of two-electron systems, particularly in the case of excited states, remains largely an open problem. The aim of the present work is to investigate the entanglement-related properties of the energy eigenstates of two exactly soluble two-electron systems: the Crandall [23] and the Hooke [20, 24, 25] atomic models. These are three-dimensional atomic models consisting of two identical, spin-$\frac{1}{2}$ fermions ('electrons') in an external harmonic confining potential, with an electron–electron interaction potential having the $r^{-2}$ form (in the case of the Crandall atom) and the standard Coulomb form in the case of the Hooke atom. We use the terms 'electrons' and 'atoms' in this paper in spite of the fact that these models can be used to describe other types of systems, such as ions in an ion trap, where the two interacting particles are ions and not electrons. In particular, it is clear that in the case of the Crandall model the inter-particle interaction does not correspond to real 'electrons'. However, as already said, we are going to follow the usual custom in the literature of referring to these systems as 'atoms' constituted by interacting 'electrons' (see, for instance, [5–7]). In this respect, we must also emphasize that the Hooke model actually does provide a useful model for a quantum dot consisting of a pair of real electrons. The helium Hamiltonian also corresponds, obviously, to a real two-electrons system.

Exactly soluble atomic models provide valuable foil systems where some fundamental aspects of atomic physics, such as the basic entanglement features exhibited by atomic states, can be studied in detail. The information gained about the eigenstates of these kind of toy models can be used as a valuable guide to interpret the properties exhibited by more realistic models such as, for example, describing helium-like atoms, quantum dots or ion traps. The study of soluble models is also useful for developing approximation techniques to treat realistic scenarios [20, 26]. Some results related to the entanglement properties of a soluble two-electron system have already been obtained for the Moshinsky model, both for the ground state [5, 6] and for excited states [7]. However, the Moshinsky system is a very special system because the interaction between the two constituent particles ('electrons') is harmonic. Here we consider the entanglement properties of the ground and the first few excited states of the two aforementioned models. Furthermore, we compute numerically the entanglement of the ground and first excited states of helium-like atoms (using high-quality eigenfunctions of the Kinoshita type [27]) and investigate its dependence on both the states' energy and the nuclear charge. Some entanglement-related aspects of helium have been considered by Gemmer and Mahler [28] in connection with the effective potential approach. However, these previous developments are unrelated to our present work, because

they involve the entanglement between the electron and the nucleus in the He$^+$ ion, here we shall investigate the entanglement between the two electrons of a neutral helium atom, regarded as two interacting, identical fermions moving in a given electrostatic potential (due to the nucleus) as described by the standard helium Hamiltonian.

The paper is organized as follows. In section 2, we provide a brief discussion of quantum entanglement in systems of two identical fermions. The Crandall and the Hooke atomic models are reviewed in section 3. Then, in sections 4 and 5, the entanglement properties of the eigenstates of these model atoms are investigated. The entanglement features of the ground and first excited states of helium-like atoms are considered in section 6. Finally, some conclusions are drawn in section 7.

## 2. Quantum entanglement in systems of two identical fermions

The Schmidt decomposition of the pure states of systems constituted by two identical fermions [29, 30] leads to a natural and physically sensible measure of the amount of entanglement exhibited by these states [30]. Given a pure state $|\Phi\rangle$ of two identical fermions there always exists an orthonormal basis $\{|i\rangle, i = 0, 1, \ldots\}$ of the single-particle Hilbert space such that $|\Phi\rangle$ can be cast as

$$|\Phi\rangle = \sum_i \sqrt{\frac{\lambda_i}{2}} (|2i\rangle|2i+1\rangle - |2i+1\rangle|2i\rangle), \tag{1}$$

where the Schmidt coefficients $\lambda_i$ verify $0 \leqslant \lambda_i \leqslant 1$ and $\sum_i \lambda_i = 1$ (if the single-particle Hilbert space has a finite dimension $N$, we assume that $N$ is even and that the sums on the index $i$ go from $i = 0$ to $i = N/2$). A useful measure of the amount of entanglement exhibited by the pure state $|\Phi\rangle$ is [30, 31]

$$\mathcal{E}(|\Phi\rangle) = 1 - \sum_i \lambda_i^2 = 1 - 2\mathrm{Tr}(\rho_1^2), \tag{2}$$

where $\rho_1 = \mathrm{Tr}_2(|\Phi\rangle\langle\Phi|)$ is the single-particle reduced density matrix obtained after tracing the two-particle density matrix $\rho = |\Phi\rangle\langle\Phi|$ over one of the particles. The entanglement measure (2) has been recently applied to the analysis of electron–electron scattering processes [32] and to the study of entanglement-related aspects of quantum brachistochrone evolutions [33].

According to the entanglement measure (2), correlations between the two fermions that are due solely to the antisymmetric character of the global two-particle state do not contribute to the entanglement of the state. Indeed, the amount of entanglement of a two-fermion state is associated with the quantum correlations exhibited by the state on top of the minimum correlations required by the antisymmetry of the global wavefunction [15, 30–36]. For example, in the case of a two-fermion state whose wavefunction can be expressed as a single Slater determinant, one of the Schmidt coefficients is equal to 1 and the rest are equal to zero. It is clear from (2) that such a state has no entanglement. In fact, there are profound physical arguments indicating that two-fermion states represented by a single Slater determinant must be regarded as non-entangled [15, 30–37]. First, the correlations exhibited by such states are not useful as a resource to perform non-classical information transmission or information processing tasks [34]. Second, the non-entangled character of states that can be represented as one Slater determinant is consistent with the possibility of assigning complete sets of properties to both parts of the composite system [35, 36].

Let us now consider the application of the above measure to a pure state of a two-electron system. For our present purposes, it is sufficient to consider states described by wavefunctions of the type

$$\Phi = \Psi(\vec{r}_1, \vec{r}_2)\chi(\sigma_1, \sigma_2), \tag{3}$$

where the global wavefunction $\Phi$ can be factorized as the product of a coordinate wavefunction $\Psi(\vec{r}_1, \vec{r}_2)$ and a spin wavefunction $\chi(\sigma_1, \sigma_2)$, $\vec{r}_1$ and $\vec{r}_2$ being the vector positions of the two electrons. The density matrix corresponding to a wavefunction of the type (3) has the form

$$\rho = \rho^{(\text{coord.})} \otimes \rho^{(\text{spin})}, \tag{4}$$

where the matrix elements of $\rho^{(\text{coord.})}$ are

$$\langle \vec{r}_1{}', \vec{r}_2{}'|\rho^{(\text{coord.})}|\vec{r}_1, \vec{r}_2\rangle = \Psi(\vec{r}_1{}', \vec{r}_2{}')\Psi^*(\vec{r}_1, \vec{r}_2). \tag{5}$$

In the case of a state with wavefunction (3) (and density matrix (4)) the entanglement measure (2) is given by

$$\mathcal{E}(|\Phi\rangle) = 1 - 2\text{Tr}\left[\left(\rho_1^{(\text{coord.})}\right)^2\right]\text{Tr}\left[\left(\rho_1^{(\text{spin})}\right)^2\right], \tag{6}$$

where $\rho_1^{(\text{coord.})}$ and $\rho_1^{(\text{spin})}$ are, respectively, the marginal density matrices obtained after computing the partial traces of the matrices $\rho^{(\text{coord.})}$ and $\rho^{(\text{spin})}$ over the degrees of freedom of one of the two particles. It is plain that the entanglement between the two electrons given by equation (6) involves both the translational and spin degrees of freedom of the electrons. To evaluate the entanglement measure (6), we have to consider separately the cases of a spin wavefunction describing parallel spins or antiparallel spins. If spins are parallel (that is, if the coordinate wavefunction is antisymmetric and the spin wavefunction is either $\chi_{++}$ or $\chi_{--}$), we have $\text{Tr}\left[\left(\rho_1^{(\text{spin})}\right)^2\right] = 1$, and the entanglement measure (2) corresponding to a two-electron state of the form (3) reduces to

$$\mathcal{E}(|\Phi\rangle) = 1 - 2\int |\langle \vec{r}_1{}'|\rho_r|\vec{r}_1\rangle|^2\, d\vec{r}_1{}'\, d\vec{r}_1, \tag{7}$$

On the other hand, if the spins are anti-parallel (that is, if the coordinate wavefunction is symmetric and the spin wavefunction is $\frac{1}{\sqrt{2}}(\chi_{+-} - \chi_{-+})$ or, alternatively, if the coordinate wavefunction is antisymmetric and the spin wavefunction is $\frac{1}{\sqrt{2}}(\chi_{+-} + \chi_{-+})$), we have $\text{Tr}\left[\left(\rho_1^{(\text{spin})}\right)^2\right] = \frac{1}{2}$, and the amount of entanglement is given by

$$\mathcal{E}(|\Phi\rangle) = 1 - \int |\langle \vec{r}_1{}'|\rho_r|\vec{r}_1\rangle|^2\, d\vec{r}_1{}'\, d\vec{r}_1. \tag{8}$$

In equations (7) and (8), we have

$$\langle \vec{r}_1{}'|\rho_r|\vec{r}_1\rangle = \int_{-\infty}^{\infty} \Psi(\vec{r}_1{}', \vec{r}_2)\Psi^*(\vec{r}_1, \vec{r}_2)\, d\vec{r}_2. \tag{9}$$

Note that a two-electron state with a wavefunction of the form

$$\frac{1}{\sqrt{2}}[\psi_1(\vec{r}_1)\psi_2(\vec{r}_2) - \psi_2(\vec{r}_1)\psi_1(\vec{r}_2)]\chi_{kk}, \qquad k = \pm, \tag{10}$$

with $\psi_1(\vec{r})$ and $\psi_2(\vec{r})$ orthogonal, normalized single-particle (coordinate) wavefunctions, has zero entanglement. This example illustrates an important point already mentioned. Wavefunction (10) is a Slater determinant. The associated correlations between the two electrons, due entirely to the anti-symmetry requirement on the fermionic state, do not contribute to the entanglement of the state.

## 3. The Crandall and the Hooke atoms

### 3.1. The Crandall atom

The Crandall 'atom' is a two-'electron' model with a harmonic confining potential and an inverse cubic electron–electron repulsion force [23]. The total Hamiltonian of the system is

$$H = -\frac{1}{2}\left(\nabla_1^2 + \nabla_2^2\right) + \frac{1}{2}\omega^2\left(r_1^2 + r_2^2\right) + \frac{\lambda}{r_{12}^2}, \tag{11}$$

where $\vec{r}_1$ and $\vec{r}_2$ are the vector positions of the two particles, $r_{12} = |\vec{r}_1 - \vec{r}_2|$, $\omega$ is the natural frequency of the external harmonic field and $\lambda$ is the interaction parameter. We have used atomic units ($m = 1, \hbar = 1$) throughout the paper. Introducing the new variables $\vec{u}$ and $\vec{v}$ [23],

$$\vec{u} = \frac{1}{\sqrt{2}}(\vec{r}_1 + \vec{r}_2), \qquad \vec{v} = \frac{1}{\sqrt{2}}(\vec{r}_1 - \vec{r}_2), \tag{12}$$

the Hamiltonian separates as

$$H = H_{\vec{u}} + H_{\vec{v}} = -\frac{1}{2}\nabla_{\vec{u}}^2 + \frac{1}{2}\omega^2 u^2 - \frac{1}{2}\nabla_{\vec{v}}^2 + \frac{1}{2}\omega^2 v^2 + \frac{\lambda}{2v^2}, \tag{13}$$

admitting the factorized eigenfunctions

$$\Psi(\vec{r}_1, \vec{r}_2) = \Psi(\vec{u}, \vec{v}) = U_{n_2 l_2 m_2}(\vec{u})V_{n_1 l_1 m_1}(\vec{v}), \tag{14}$$

with

$$U_{n_2 l_2 m_2}(\vec{u}) = \mathrm{e}^{-\frac{\omega u^2}{2}} u^{l_2} L_{n_2}^{l_2 + \frac{1}{2}}(\omega u^2) Y_{l_2 m_2}(\theta_u, \phi_u), \tag{15}$$

and

$$V_{n_1 l_1 m_1}(\vec{v}) = \mathrm{e}^{-\frac{\omega v^2}{2}} v^a L_{n_1}^{a + \frac{1}{2}}(\omega v^2) Y_{l_1 m_1}(\theta_v, \phi_v), \tag{16}$$

where $L_n^\alpha(x)$ denote the Laguerre polynomials and $a = \frac{1}{2}[\sqrt{1 + 4\lambda + 4l_1(l_1 + 1)} - 1]$. The variables $u, \theta_u, \phi_u, v, \theta_v, \phi_v$ are the spherical coordinates associated with the vectors $(\vec{u}, \vec{v})$. We will denote by $|n_1 l_1 m_1 n_2 l_2 m_2\rangle_{\vec{u}, \vec{v}}$ the (spatial) eigenfunctions of the Hamiltonian (11), which are characterized by the quantum numbers $n_1$, $l_1$, $m_1$, $n_2$, $l_2$ and $m_2$ (to fully define the eigenstates of the two-electron system, we have to specify also the spin wavefunction $\xi(\sigma_1, \sigma_2)$). The above quantum numbers adopt the values

$$\begin{aligned} n_1, l_1 &= 0, 1, 2, 3, \ldots & m_1 &= -l_1, \ldots, l_1, \\ n_2, l_2 &= 0, 1, 2, 3, \ldots & m_2 &= -l_2, \ldots, l_2, \end{aligned} \tag{17}$$

and the corresponding eigenenergies are [23]

$$E = \frac{\omega}{2}\{5 + 4n_2 + 4n_1 + 2l_2 + [1 + 4\lambda + 4l_1(l_1 + 1)]^{\frac{1}{2}}\}. \tag{18}$$

All the (coordinate) wavefunctions $|n_1 l_1 m_1 n_2 l_2 m_2\rangle_{\vec{u}, \vec{v}}$ have definite parity, which is determined by the quantum number $l_2$: even values of $l_2$ correspond to symmetric coordinate eigenfunctions and odd values of $l_2$ to antisymmetric ones. A final remark concerning our notation is in order. A cursory glance at the ket $|n_1 l_1 m_1 n_2 l_2 m_2\rangle_{\vec{u}, \vec{v}}$ may suggest that it represents a separable state. However, in general, it represents an entangled state of the two-electron system. Indeed, these wavefunctions are the product of two functions, one depending on the centre of mass' coordinates and the other on the relative coordinates of the two electrons, and these products are not in general expressible as a single Slater determinant. As we shall see in the next section, the same occurs in the case of the Hooke model.

### 3.2. The Hooke atom

The Hooke atom is a two-electron atomic model with harmonic confining potential and Coulombic electron–electron repulsion force. The total Hamiltonian of the system is

$$H = -\frac{1}{2}\left(\nabla_1^2 + \nabla_2^2\right) + \frac{1}{2}\omega^2\left(r_1^2 + r_2^2\right) + \frac{1}{r_{12}}, \tag{19}$$

where $\vec{r}_1$ and $\vec{r}_2$ are the coordinates of the two particles, $r_{12} = |\vec{r}_1 - \vec{r}_2|$ and $\omega$ is the natural frequency of the external harmonic field. Introducing the centre of mass and the relative position vectors [25]

$$\vec{R} = \tfrac{1}{2}(\vec{r}_1 + \vec{r}_2) \qquad \vec{r} = \vec{r}_1 - \vec{r}_2, \tag{20}$$

the Hamiltonian separates as follows:

$$H = H_{\vec{R}} + H_{\vec{r}} = -\frac{1}{4}\nabla_{\vec{R}}^2 + \omega^2\vec{R}^2 - \nabla_{\vec{r}}^2 + \frac{1}{4}\omega^2 r^2 + \frac{1}{r}. \tag{21}$$

The eigenfunctions of (21) can be factorized as

$$\Psi(\vec{r}_1, \vec{r}_2) = \Psi(\vec{R}, \vec{r}) = \psi_{n_1,l_1,m_1}(\vec{R})\phi_{n_2,l_2,m_2}(\vec{r}), \tag{22}$$

leading to the pair of eigenvalue equations

$$\left[-\tfrac{1}{2}\nabla_R^2 + \tfrac{1}{2}\omega_R^2 R^2\right]\psi(\vec{R}) = \eta'\psi(\vec{R}), \tag{23}$$

and

$$\left[-\frac{1}{2}\nabla_r^2 + \frac{1}{2}\omega_r^2 r^2 + \frac{1}{2r}\right]\phi(\vec{r}) = \epsilon'\phi(\vec{r}), \tag{24}$$

with $\omega_R = 2\omega$ and $\omega_r = \frac{1}{2}\omega$. The total energy of eigenstate (22) is then $E = \eta + \epsilon$, where $\eta = \frac{1}{2}\eta'$ and $\epsilon = 2\epsilon'$.

Equation (23) is the eigenvalue equation corresponding to a three-dimensional, isotropic quantum harmonic oscillator, with well-known solutions of the form

$$\psi(\vec{R}) = N_{n_1,l_1} R^l\, e^{\frac{-\omega_R^2 R^2}{2}} L_{n_1}^{(l_1+1/2)}(\omega R^2) Y_{l_1,m_1}(\theta_R, \phi_R), \tag{25}$$

with

$$N_{n_1,l_1} = \left(\left(\frac{\omega_R^3}{4\pi}\right)^{\frac{1}{2}} \frac{2^{n_1+2l_1+3} n_1!(\omega_R/2)^l}{(2n_1 + 2l_1 + 1)!!}\right)^{\frac{1}{2}} \tag{26}$$

and

$$\eta' = \omega_R\left(2n_1 + l_1 + \tfrac{3}{2}\right). \tag{27}$$

On the other hand, the eigenvalue equation (24) admits a closed analytical solution only for certain particular states, each of them requiring a separate treatment. These analytical solutions can be determined by recourse to a power-series expansion with a three-step recurrence in the quantum number $n_2$. The lowest energy state that can be calculated by this method corresponds to $n_2 = 2$. For $n_2 = 2$ and arbitrary $l_2, m_2$, the wavefunction is given by

$$\phi(\vec{r}) = k_2 r^{l_2}\, e^{-\frac{r^2}{8(l_2+1)}}\left(1 + \frac{r}{2(l_2 + 1)}\right) Y_{l_2,m_2}(\theta_r, \phi_r), \tag{28}$$

where

$$k_2 = \left[2^{1+2l_2}(1 + l_2)^{l_2}\left(\sqrt{l_2 + 1}(5 + 4l_2)\Gamma\left(\tfrac{3}{2} + l_2\right) + 4(l_2 + 1)\Gamma(2 + l_2)\right)\right]^{-\frac{1}{2}}. \tag{29}$$
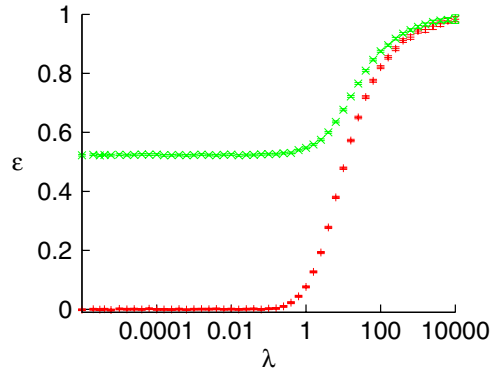
**Figure 1.** Entanglement of the ground (labelled by 000000) and first excited state (labelled by 100000), with anti-parallel spins of the Crandall atom as a function of the parameter $\lambda$.

The concomitant eigenvalue is

$$\epsilon' = \frac{2l_2 + 5}{8(l_2 + 1)}. \tag{30}$$

By recourse to solution (28), we can build the full wavefunctions for the states $(n_1, l_1, m_1, n_2 = 2, l_2, m_2)$ with $\omega = \frac{1}{2(l_2+1)}$. For $n_2 = 3$ and arbitrary $l_2, m_2$, one has that

$$\phi(\vec{r}) = k_3 r^{l_2} \, e^{-\frac{r^2}{8(4l_2+5)}} \left(1 + \frac{r}{2(l_2+1)} + \frac{r^2}{4(l_2+1)(4l_2+5)}\right) Y_{l_2,m_2}(\theta_r, \phi_r) \tag{31}$$

with

$$k_3 = \frac{1}{16} \left[ \frac{2^{7+2l_2}(3+2l_2)(5+4l_2)^{2+l_2}\Gamma(1+l_2)}{1+l_2} \right. $$
$$\left. + \frac{4^{2+l_2}(5+4l_2)^{3/2+l_2}(61+88l_2+32l_2^2)\Gamma(3/2+l_2)}{(1+l_2)^2} \right]. \tag{32}$$

The associated eigenvalue is

$$\epsilon' = \frac{2l_2 + 7}{8(4l_2 + 5)}. \tag{33}$$

Using (31), we can build the complete wavefunctions for the states $(n_1, l_1, m_1, n_2 = 3, l_2, m_2)$ with $\omega = \frac{1}{2(4l_2+5)}$. Heretoforth we will denote by $|n_1 l_1 m_1 n_2 l_2 m_2\rangle_{\vec{r},\vec{R}}$ the eigenfunctions of the Hamiltonian (19), which are characterized by the quantum numbers $n_1, l_1, m_1, n_2, l_2$ and $m_2$. To fully define the eigenstates of the two-electron system, we have to specify, of course, also the spin wavefunction $\chi(\sigma_1, \sigma_2)$.

## 4. Entanglement in the Crandall atom

The integrals appearing in equations (7)–(9), that have to be computed in order to evaluate the amount of entanglement of the eigenstates, cannot be computed analytically for general eigenstates of the Crandall model. We have evaluated these integrals by recourse to the Monte Carlo method. The main results obtained are summarized in figures 1–4.
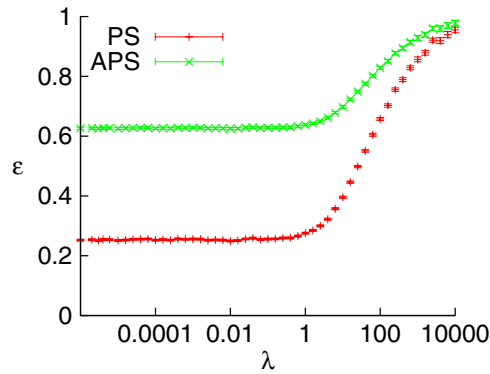
**Figure 2.** Entanglement of the ($n = l = 1$ and all the other quantum numbers equal to 0)-eigenstates, with parallel (PS) and anti-parallel spins (APS) of the Crandall atom as a function of the parameter $\lambda$.
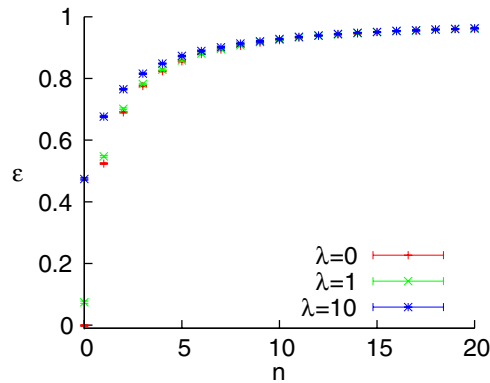


**Figure 3.** Entanglement as a function of the quantum number $n$ corresponding to the eigenstates having all the other quantum numbers equal to zero, for three different values of the parameter $\lambda$.

We encounter two general trends. First, the entanglement increases monotonically with the parameter $\lambda$ and, consequently, with the strength of the interaction between the particles. For high enough values of $\lambda$, the entanglement approaches its maximum value $\mathcal{E} = 1$. Second, the amount of entanglement also tends to increase when we consider higher excited states (that is, it increases with the energy).

Another interesting feature observed in figures 1 and 2 is that the entanglement exhibited by excited eigenstates does not necessarily go to zero in the limit $\lambda \rightarrow 0$. In other words, *for an arbitrarily weak (but finite) interaction, there are already excited eigenstates exhibiting a considerable amount of entanglement.* In the non-interacting case corresponding to $\lambda = 0$, these states have degenerate eigenenergies and the degeneracy enables one to construct an alternative set of non-entangled eigenstates sharing the same energy. However, when $\lambda > 0$, the interaction lifts the degeneracy and the aforementioned eigenstates become necessarily entangled. It is worth stressing that the finite amount of entanglement corresponding to the limit $\lambda \rightarrow 0$ is not due to the correlations arising exclusively from the antisymmetric nature of the (global) fermionic states. As already mentioned, these correlations do not contribute
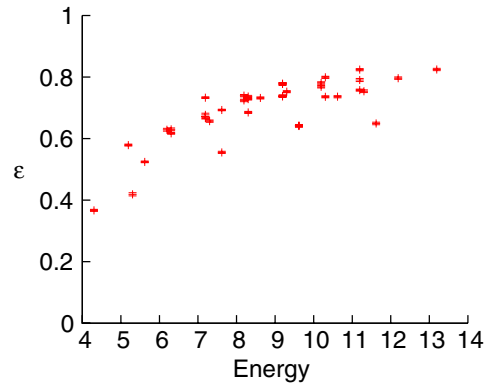
**Figure 4.** Entanglement for the ground state and some excited states of the Crandall model as a function of the energy of the system in the $\lambda \to 0$ limit. The states represented correspond to $m_1 = m_2 = 0$ and the remaining four quantum numbers adopting all the possible combinations of values within the range $0 \leqslant n_1, l_1, n_2, l_2 \leqslant 2$.

to the entanglement of the state. As can be appreciated in figure 4, in the limit $\lambda \to 0$, the amount of entanglement tends to increase with the energy of the eigenstates.

## 5. Entanglement in the Hooke atom

As in the case of the Crandall model, integrals (7)–(9) needed to determine the amount of entanglement of the systems' eigenstates do not admit analytical treatment and we evaluated them using a Monte Carlo approach similar to the one used in the calculations for the Crandall model. The entanglement properties exhibited by the eigenstates of the Hooke atom are similar to those characterizing the eigenstates of the Crandall model.

The entanglement of several eigenstates of the Hooke model with $\omega = \frac{1}{2}$ is depicted in figures 5 and 6 against the corresponding eigenenergies. The states represented are characterized by $n_2 = 2$, $l_2 = 0$, $m_1 = m_2 = 0$, and several different values of the quantum numbers $n_1, l_1$. It can be appreciated in these figures that, as happens with the Crandall model, the entanglement of the eigenstates of the Hooke atom also tends to increase with the eigenstates' energy. This is particularly evident in figure 5, where the entanglement exhibits a tendency to increase both with $n_1$ and $l_1$ (note that in the Hooke model the energy is an increasing function of both these numbers). The increasing behaviour of entanglement with energy is also observed in figure 6, where the states with all combinations of the quantum numbers $n_1$ and $l_1$ corresponding to $\frac{\eta'}{\omega_R} \leqslant 16.5$ are represented.

The increasing behaviour of entanglement with energy may at first sight seem counterintuitive. This idea is probably due to the fact that the two particles constituting the system tend to separate from each other as the energy of the eigenstates increase. It must be stressed, however, that the quantum entanglement and the spatial separation between two particles are completely unrelated physical concepts. Two quantum particles may be highly entangled no matter how large is the average distance between them. The large amount of entanglement exhibited by highly excited states may also seem to contradict the fact that these states yield a semiclassical description. However, even if some aspects of these eigenstates are indeed describable by a semiclassical approach, these states do still exhibit fundamental
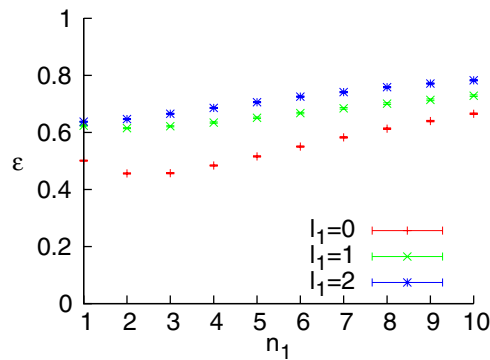
**Figure 5.** Entanglement of the ground state and several excited states of the Hooke atom (with $\omega = \frac{1}{2}$) as a function of the energy of the system. The eigenstates depicted correspond to $n_2 = 2$, $l_2 = 0$, $m_2 = 0$, $l_1 = 0, 1, 2$, $m_1 = 0$, and several different values of the quantum numbers $n_1$.
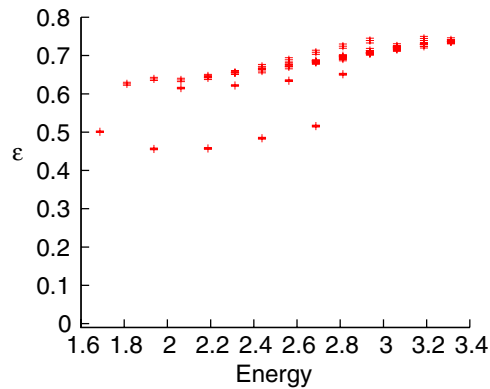


**Figure 6.** Entanglement of the ground state and several excited states of the Hooke atom (with $\omega = \frac{1}{2}$) as a function of the energy of the system. The eigenstates depicted correspond to $n_2 = 2$, $l_2 = 0$, $m_1 = m_2 = 0$ and all the values of the quantum numbers $n_1$ and $l_1$ consistent with $\frac{\eta'}{\omega_R} \leqslant 16.5$.

quantum features[5]. Therefore, the tendency of entanglement to increase with energy, while being an interesting feature of the systems considered here that certainly deserves further elucidation, should not necessarily be regarded as counterintuitive. In this regard, it is worth to mention that the observed connection between entanglement and energy is fully consistent with a well-known fact in atomic physics: the Hartree–Fock approximation (which is actually a zero-entanglement approximation) tends to deteriorate as one considers higher excited states of a multi-electron atomic system.

---

[5] In fact, there exist fundamental quantum features that are exhibited by all quantum states, pure or mixed. An interesting example is provided by the violation of the Cabello inequalities associated with quantum contextuality [38, 39].

**Table 1.** Energies for the wavefunction of helium-like atoms. GS means the $1s^2$ $^1$S ground state.

| $Z$ | State | Energy |
|---|---|---|
| 1 | GS | $-0.527\,751\,016\,5226$ |
| 2 | GS | $-2.903\,724\,377\,032$ |
| 2 | 1s2s,2 $^3$S | $-2.175\,229\,378\,225$ |
| 2 | 1s2s,2 $^1$S | $-2.145\,974\,045\,970$ |
| 3 | GS | $-7.279\,913\,412\,667$ |
| 4 | GS | $-13.655\,566\,238\,41$ |
| 5 | GS | $-22.030\,971\,580\,23$ |

## 6. Entanglement in helium-like atoms

It is interesting to explore to what extent the main entanglement features characterizing the exactly soluble models of Crandall and Hooke are also observed in systems whose confining potential is not harmonic. As a first step in this direction, we are now going to compute the entanglement corresponding to the ground and first excited states of helium-like atoms by means of the high-quality eigenfunctions of the Kinoshita type obtained by Koga [27].

The Hamiltonian of an helium-like atom (in atomic units) reads

$$H = -\frac{1}{2}\nabla_1^2 - \frac{1}{2}\nabla_2^2 - \frac{Z}{r_1} - \frac{Z}{r_2} + \frac{1}{r_{12}}, \tag{34}$$

where $Z$ denotes the nuclear charge. The aforementioned eigenfunctions for helium-like systems are represented by the following Kinoshita-type Ansatz with half-integer powers [27]:

$$\Psi_N = e^{-\xi s} \sum_{i=1}^{N} c_i s^{\frac{l_i}{2}} \left(\frac{t}{u}\right)^{m_i} \left(\frac{u}{s}\right)^{\frac{n_i}{2}}, \tag{35}$$

where $s$, $t$ and $u$ stand for the Hylleraas coordinates given by

$$\begin{aligned} s &= |\vec{r}_1| + |\vec{r}_2| & t &= |\vec{r}_1| - |\vec{r}_2| & u &= |\vec{r}_1 - \vec{r}_2| \\ s &\in [0, \infty], & u &\in [0, s], & t &\in [-u, u]. \end{aligned} \tag{36}$$

The optimization of the exponent $\xi$, the coefficients $c_i$ and the powers $\{l_i, m_i, n_i\}$ in the eigenfunctions given by equation (35) with $N = 100$ terms leads to the energies listed in table 1.

The main results obtained here concerning the entanglement-related features of helium-like atoms are summarized in figures 7 and 8. Our findings for the helium-like atoms are fully consistent with the entanglement properties of the Crandall and Hooke models that were discussed in the previous sections. Indeed, the data depicted in figure 7 suggest that the entanglement of the helium eigenstates tends to increase with energy. On the other hand, figure 8 clearly shows that the entanglement of the ground state of helium-like systems decreases monotonically with the nuclear charge $Z$. This last parameter determines the strength of the nuclear Coulomb field, while the strength of the electron–electron interaction is constant. Consequently, the behaviour observed in figure 8 can be construed as indicating that the system becomes more entangled when the relative strength of the electron–electron interaction (as compared with the nuclear–electron interaction) increases. This behaviour is similar to those exhibited by both the Crandall and Hooke atomic models.
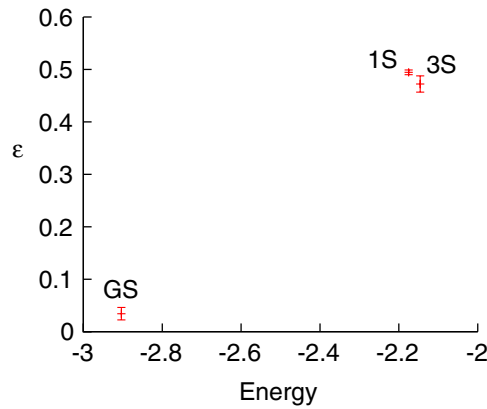
**Figure 7.** Entanglement of the ground and first excited states of the helium atom as a function of the energy.
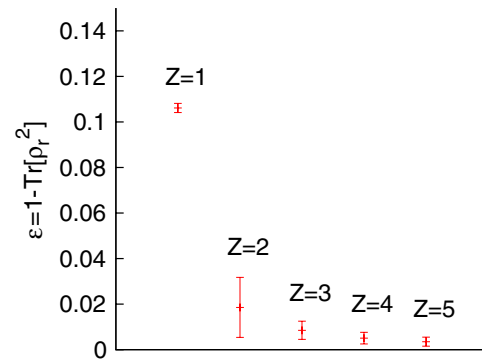


**Figure 8.** Entanglement of the ground states of helium-like atoms for different values of the nuclear charge Z.

## 7. Conclusions

We have explored the entanglement-related properties of two two-electron atomic models: the Crandall and Hooke atoms. We have considered particular values of the Hamiltonian parameters and eigenstates' quantum numbers that allow for exact solutions of the corresponding Schrödinger eigenvalue equation. Even though we have analytical expressions for the models' eigenfunctions, the associated amounts of entanglement have to be computed numerically.

The main entanglement features exhibited by the eigenstates of the Crandall and Hooke atoms are similar. In both cases the behaviour of the entanglement associated with the eigenstates of the system obeys the same general patterns. The amount of entanglement of the eigenstates tends to increase with the corresponding eigenenergy. This is consistent with the trends observed in the Moshinsky model [7] and also in the one-dimensional helium-like system investigated by Carlier *et al* [8]. The entanglement in the Crandall model also tends to increase with the relative strength of the electron–electron interaction (as compared with the strength of the confining harmonic potential) approaching its maximum when the

interaction becomes large enough. On the other hand, when the interaction tends to zero (but is still finite), the entanglement of the eigenstates does not necessarily go to zero. There are eigenstates endowed with a finite amount of entanglement for arbitrarily weak (but non-vanishing) interaction.

It would be interesting to explore systematically the entanglement properties of other models, not confined within a harmonic well, in order to determine which (if any) of the above trends are shared by general two-particle systems and which are the special properties characterizing models with an external harmonic confining potential. As a first step towards this goal, we have studied the entanglement of the ground and first excited states of helium-like atoms. We found that the entanglement exhibited by the eigenfunctions of helium-like atoms tends to increase with energy and decrease with the nuclear charge $Z$. Any new developments along these lines of enquiry will be very welcome.

## Acknowledgments

## References

[1] Das C and Bhattacharyya K 2009 *Phys. Rev. A* **79** 012107
[2] Lopez-Rosa S, Antolin J, Angulo J C and Esquivel R O 2009 *Phys. Rev. A* **80** 012505
[3] Gonzalez-Ferez R and Dehesa J S 2003 *Phys. Rev. Lett.* **91** 113001
[4] Sen K D, Antolin J and Angulo J C 2007 *Phys. Rev. A* **76** 032502
[5] Pipek J and Nagy I 2009 *Phys. Rev. A* **79** 052501
[6] Amovilli C and March N H 2004 *Phys. Rev. A* **69** 054302
[7] Yañez R J, Plastino A R and Dehesa J S 2010 *Eur. Phys. J. D* **56** 141
[8] Carlier F, Mandilara A and Sarfati A 2007 *J. Phys. B: At. Mol. Opt. Phys.* **40** S199
[9] Dehesa J S, Gonzalez-Ferez R and Sanchez-Moreno P 2007 *J. Phys. A: Math. Theor.* **40** 1845
[10] Nagy A 2007 *Chem. Phys. Lett.* **449** 212
[11] Nagy A 2006 *Chem. Phys. Lett.* **425** 154
[12] Glasser M L and Nieto L M 2005 *J. Phys. A: Math. Gen.* **38** L455
[13] Bengtsson I and Zyczkowski K 2006 *Geometry of Quantum States: An Introduction to Quantum Entanglement* (Cambridge: Cambridge University Press)
[14] Nielsen N and Chuang I L 2000 *Quantum Computation and Quantum Information* (Cambridge: Cambridge University Press)
[15] Amico L, Fazio L, Osterloh A and Vedral V 2008 *Rev. Mod. Phys.* **80** 517
[16] Aquilanti V, Bitencourt A C P, Ferreira C D S, Marzuoli A and Ragni M 2008 *Phys. Scr.* **78** 058103
[17] Luo S and Zhang Z 2003 *Phys. Lett. A* **315** 189
[18] Gemmer J, Michel M and Mahler G 2004 *Quantum Thermodynamics* (Berlin: Springer)
[19] Schlosshauer M 2007 *Decoherence and the Quantum-to-Classical Transition* (Berlin: Springer)
[20] Coe J P, Sudbery A and D'Amico I 2008 *Phys. Rev. B* **77** 205122
[21] Osenda O and Serra P 2008 *J. Phys. B: At. Mol. Opt. Phys.* **41** 065502
[22] Ferrón A, Osenda O and Serra P 2009 *Phys. Rev. A* **79** 032509
[23] Crandall R, Whitnall R and Bettega R 1984 *Am. J. Phys.* **52** 438
[24] Ludeña E V, Gomez D, Karasiev V and Nieto P 2004 *Int. J. Quantum Chem.* **99** 297
[25] Taut M 1993 *Phys. Rev. A* **48** 3561
[26] Amovilli C and March N H 2003 *Phys. Rev. A* **67** 022509
[27] Koga T 1996 *J. Chem. Phys.* **104** 6308
[28] Gemmer J and Mahler G 2002 *Europhys. Lett.* **59** 159
[29] Schliemann J, Cirac J I, Kus M, Lewenstein M and Loss D 2001 *Phys. Rev. A* **64** 022303

[30] Naudts J and Verhulst T 2007 *Phys. Rev.* A **75** 062104
[31] Plastino A R, Manzano D and Dehesa J S 2009 *Europhys. Lett.* **86** 20005
[32] Buscemi F, Bordone P and Bertoni A 2007 *Phys. Rev.* A **75** 032301
[33] Borras A, Plastino A R, Casas M and Plastino A 2008 *Phys. Rev.* A **78** 052104
[34] Eckert K, Schliemann J, Bruss D and Lewenstein M 2002 *Ann. Phys.* **299** 88
[35] Ghirardi G and Marinatto L 2004 *Phys. Rev.* A **70** 012109
[36] Ghirardi G, Marinatto L and Weber T 2002 *J. Stat. Phys.* **108** 49
[37] Oliveira V C G, Santos H A B, Torres L A M and Souza A M C 2008 *Int. J. Quantum Inf.* **6** 379
[38] Cabello A 2008 *Phys. Rev. Lett.* **101** 210401
[39] Kirchmair G, Zahringer F, Gerritsma R, Kleinmann M, Guhne, Cabello A and Blatt R 2009 *Nature* **460** 494